DOI: 10.1002/ejic.200600294

A Route to Multi-Clusters Containing Half-Sandwich Rh and Ir Complexes of Chelating 1,2-Dicarba-*closo*-dodecaborane(12)-1,2-dithiolate Ligands

Jian-Qiang Wang,[a] Chun-Xia Ren,[a] and Guo-Xin Jin*[a]

Dedicated to Professor Max Herberhold on the occasion of his 70th birthday

Keywords: Iridium / Rhodium / Carboranes / N ligands / Cluster compounds

Reaction of the 16-electron half-sandwich rhodium and iridium complexes [Cp*M{$S_2C_2(B_{10}H_{10})$}] [M = Rh (**1a**), Ir (**1b**)] with multidentate ligands (L) such as 5,10,15,20-tetra(4-pyridyl)porphyrin) (H_2TPyP), 2,4,6-tri(4-pyridyl)-1,3,5-triazine (tpt), and 4,4′-azopyridine, gave the corresponding multicluster complexes [Cp*$MS_2C_2(B_{10}H_{10})]_n$(L) [M = Rh, Ir; n = 4, L = H_2TPyP (**2**); 3, L = tpt (**3**); 2, L = 4,4′-azopyridine (**4**), *N*,*N*′-bis(4-pyridinylmethylene)biphenyl-4,4′-diamine (**5**), pyrazine, (**6**), 2,5-di(4-pyridyl)-1,3,4-oxadiazole (**7**), 1,2-di(4-pyridyl)ethylene) (**8**), diisonicotinic acid 1,4-phenylene diester (**9**), 4,4′-bipyridine (**10**)]. The X-ray structure of **2a** reveals that an H_2TPyP unit bridges four [Cp*$RhS_2C_2(B_{10}H_{10})$] fragments to form a tetranuclear [Cp*$RhS_2C_2(B_{10}H_{10})]_4$($H_2$TPyP) complex and the [Cp*$RhS_2C_2(B_{10}H_{10})$] units adopt a tail-to-tail contact mode, rather than a head-to-tail mode, in spite of the large steric repulsion between the two carborane ligands. In complex **3a**, three [Cp*$RhS_2C_2(B_{10}H_{10})$] units are symmetrically arranged around the periphery of one tpt core, thus forming a "bowl-shaped" structure. In **4a**, **5a**, **6a**, **8b**, and **9b**, two [Cp*$RhS_2C_2(B_{10}H_{10})$] fragments take a *trans* conformation around the linear or pseudo-linear pyridyl-based ligand core, while in **7a** they are in a *cis* conformation. All new complexes **2**–**10** were characterized by ^{1}H and ^{11}B NMR spectroscopy, and X-ray structural analyses are reported for complexes **2a**, **3a**, **4a**, **5a**, **6a**, **7a**, **8b**, and **9b**.

Introduction

During the last decade, a series of mononuclear 16-electron Cp* half-sandwich complexes of Co, Rh, and Ir have been prepared that contain didentate, chelating 1,2-dicarba-*closo*-dodecaborane(12)-1,2-dichalcogenolate ligands $[(B_{10}H_{10})C_2E_2]^{2-}$ (E = S, Se).[1] These complexes exhibit a rich coordination chemistry due to both their unsaturation at the metal atom and the bridging or chelating properties of the sulfur or selenium atoms.[2] Among the types of target structures attracting attention are highly symmetrical, aesthetically appealing architectures such as star-shaped molecules.[3] The efforts to build cluster-supported molecular or supramolecular structures are expected to offer many fascinating research problems with potentially significant ramifications.[4] To the best of our knowledge, only a few examples of *ortho*-carboranyl-functionalized highly branched molecules have been reported in the search for efficient methods for assembling suitable organic or inorganic linkers into desired target metallodendrimers.[5–7] Carboranes are obvious candidates for such applications because of their synthetic versatility and well-developed derivative chemistry. Our laboratory and Herberhold et al. have already reported the synthesis of the 16-electron "pseudo-aromatic" half-sandwich complexes [Cp*M{$E_2C_2(B_{10}H_{10})$}] (M = Co, Rh, Ir; E = S, Se),[8] and a recent publication from our laboratory suggests that this species may be promising for further transformations owing to its electron deficiency at the metal center.[9] This has allowed the construction of a polycarborane molecular architecture that takes advantage of special attributes, such as an addition reaction at the metal center in a dichalcogenolato metal heterocycle.[8]

Here, we describe the assembly of soluble, air-stable supramolecular structures based on the metal-containing moieties [Cp*M{$S_2C_2(B_{10}H_{10})$}] (M = Rh **1a**; M = Ir **1b**), bridged by nitrogen-based, star-shaped organic spacers (Scheme 1).

[a] Shanghai Key Laboratory of Molecular Catalysis and Innovative Material, Department of Chemistry, Fudan University, Shanghai 200433, P. R. China
Fax: +86-21-6564-3776
E-mail: gxjin@fudan.edu.cn

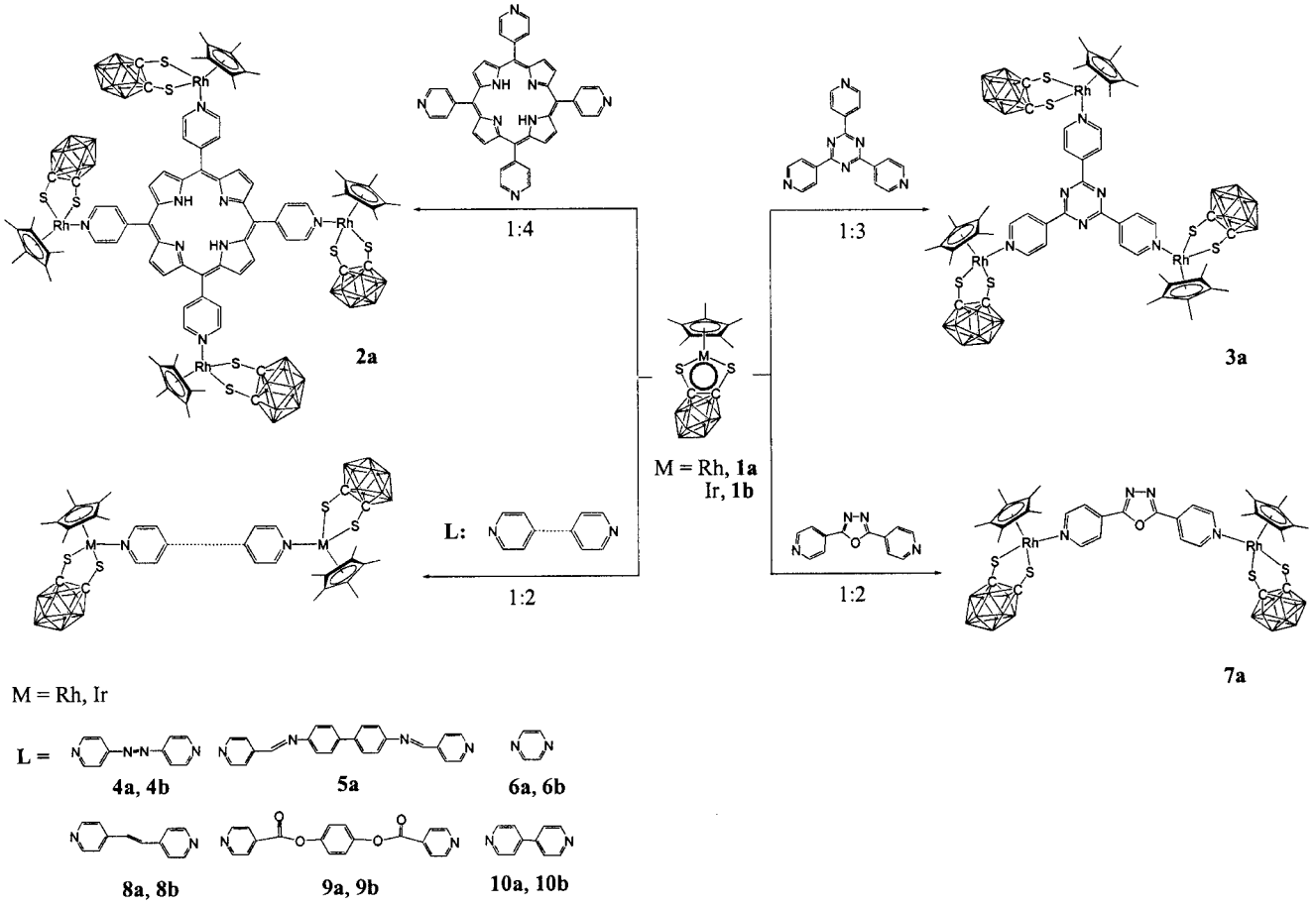

Scheme 1. Reaction of $[Cp^*MS_2C_2(B_{10}H_{10})]$ with a pyridyl-based ligand to give complexes **2**–**10**.

Results and Discussion

Synthesis and Characterization

We recently reported the reaction of the iridium precursor $[Cp^*IrS_2C_2(B_{10}H_{10})]$ (**1b**) with 2,4,6-tri(4-pyridyl)-1,3,5-triazine (tpt) and 4,4′-bipyridine, which leads to the formation of the multi-cluster $[Cp^*IrS_2C_2(B_{10}H_{10})]_n(L)$ [n = 3, L = tpt; 2, L = 4,4′-bipyridine].[6] By using different metal complexes (**1a**, **1b**) and the linear or pseudo-linear pyridyl-based ligand that have been used as building blocks for discrete supramolecular assemblies[10] as starting materials, further neutral star-shaped molecules with $[Cp^*MS_2C_2(B_{10}H_{10})]$ (M = Rh or Ir) units can be synthesized. Scheme 1 shows the formation of star-shaped molecules **2**–**10**, which were characterized by single-crystal X-ray analysis, elemental analysis, and ^{1}H NMR, ^{11}B NMR and IR spectroscopy.

Stirring a mixture of $[Cp^*Rh\{S_2C_2(B_{10}H_{10})\}]$ (**1a**) and 5,10,15,20-tetra(4-pyridyl)porphyrin (H_2TPyP) in CH_2Cl_2 at room temperature for 24 h produced a red solution of **2a** in high yield. The IR spectrum shows a strong band at approximately 2559 cm^{-1} due to the carborane group. The formation of **2a** was confirmed by the appearance of signals at δ = –2.89, 1.78, 8.20, 9.02, and 9.38 ppm in the ^{1}H NMR spectrum, which are ascribed to the H_2TPyP and Cp* ligands; the ^{11}B NMR spectrum exhibits carborane (B–H) resonances at δ = –5.8, –8.2, –9.0, and –10.8 ppm.

Trinuclear complex **3a**, formulated as $[Cp^*Rh\{S_2C_2(B_{10}H_{10})\}]_3(tpt)$ from elemental analysis and ^{1}H NMR spectroscopy, was formed when **1a** was treated with tpt in a 3:1 molar ratio in CH_2Cl_2 at room temperature (Scheme 1). The ^{1}H NMR spectrum shows two kinds of resonances for each of the Cp* and tpt ligands, at δ = 1.77 ppm and δ = 8.67, 8.96 ppm respectively, suggesting the presence of configurational isomers. The signals at δ = –7.9 and –10.3 ppm in the ^{11}B NMR spectrum suggest B–H activation.

The 16-electron "pseudo-aromatic" half-sandwich complexes **1a** and **1b** react readily with two equivalents of 4,4′-azopyridine to give dimeric complexes formulated as $[Cp^*M\{S_2C_2(B_{10}H_{10})\}]_2(C_{10}H_8N_4)$ (M = Rh **4a**, Ir **4b**). The IR spectra of **4a** and **4b** show B–H bands for the carboranes at 2568 and 2562 cm^{-1}, respectively. The ^{1}H NMR spectrum of **4a** shows a singlet at δ = 1.77 ppm due to the methyl groups of the Cp* ligands and resonances at about δ = 7.76 and 8.85 ppm due to the 4,4′-azopyridine protons; that for **4b** has a singlet at δ = 1.87 and δ = 7.80 and 8.92 ppm. The ^{11}B NMR spectrum exhibits a carborane (B–H) resonance at δ = –6.1, –7.5, –8.7, and –10.9 ppm for **4a** and δ = –6.2, –7.5, –8.6, and –10.5 ppm for **4b**. Detailed structures were confirmed by X-ray analysis of **4a** (see below), which re-

vealed that the complex is a dimer bridged by a 4,4′-azopyridine molecule.

Analogously, treatment of **1a** or **1b** with *N*,*N*′-bis(4-pyridinylmethylene)biphenyl-4,4′-diamine, pyrazine, 2,5-di(4-pyridyl)-1,3,4-oxadiazole, 1,2-di(4-pyridyl)ethylene, diisonicotinic acid 1,4-phenylene diester, or 4,4′-bipyridine also generated the dinuclear complexes $[Cp^*Rh\{S_2C_2(B_{10}H_{10})\}]_2(C_{24}H_{18}N_4)$ (**5a**), $[Cp^*M\{S_2C_2(B_{10}H_{10})\}]_2(C_4H_4N_2)$ (M = Rh **6a**, Ir **6b**), $[Cp^*Rh\{S_2C_2(B_{10}H_{10})\}]_2(C_{12}H_8N_4O)$ (**7a**), $[Cp^*M\{S_2C_2(B_{10}H_{10})\}]_2(C_{12}H_{10}N_2)$ (M = Rh **8a**, Ir **8b**), $[Cp^*Rh\{S_2C_2(B_{10}H_{10})\}]_2(C_{18}H_{12}N_2O_4)$ (M = Rh **9a**, Ir **9b**), $[Cp^*M\{S_2C_2(B_{10}H_{10})\}]_2(C_{10}H_8N_2)$ (M = Rh **10a**, Ir **10b**), respectively. All the ^1H NMR spectra in $CDCl_3$ show two resonances for each of the Cp* and pyridyl or pyrazine ligands and the ^{11}B NMR spectra in $CDCl_3$ exhibit a carborane (B–H) resonance. In the IR spectra, the B–H vibration bands of the carborane group appear at 2575–2580 cm^{-1} for all of the complexes, and the C=O band appears at 1690 cm^{-1} for **9a** and 1692 cm^{-1} for **9b**.

Molecular Structures

The crystal structure of **2a** consists of quadridentate units in which there are two crystallographically independent Rh^{III} atoms and the H_2TPyP ligand adopts a bridging mode (Figure 1, a). All of the rhodium centers adopt a three-legged piano-stool conformation with a six-coordinate geometry, assuming that the Cp* ligand functions as a three-coordinate ligand. The angles between adjacent atoms around the rhodium atoms are nearly 90°. All of the Cp* atoms fall in a fairly good plane, and the Cp* ligands are symmetrically bound to the rhodium atoms. The distances between Rh and the least-squares plane of the Cp* ring are 1.78 and 1.82 Å, which compare well with those for other rhodium complexes containing Cp*.[11,12] The dihedral angle along the S···S vector in the rhodadithiolato metallacycle (RhS_2C_2) is about 173° and 169°, compared to 180° in **1a**.[8b] An H_2TPyP unit bridges four $[Cp^*RhS_2C_2(B_{10}H_{10})]$ fragments to form the tetranuclear $[Cp^*RhS_2C_2(B_{10}H_{10})]_4(H_2TPyP)$ complex. An interesting feature of this solid-state structure is that the $[Cp^*RhS_2C_2(B_{10}H_{10})]$ units adopt a tail-to-tail contact mode, rather than a head-to-tail mode, in spite of the large steric repulsion between the two carborane ligands, similar to that reported previously.[5] In the crystal lattice, molecules of **2a** form an extended two-dimensional layered structure. Within each layer, the molecules of **2a** interdigitate through the four legs, as depicted inpart b of Figure 1. The dihedral angle between neighboring porphyrins is 46.8°. The shortest distance between Cp* ligands in the same layer is 3.75 Å, and there is a very weak π–π interaction between the molecules. In addition, four dendrimer complexes in the same layer form a parallelogram with dimensions 15.4×18.0 $Å^2$. As illustrated in Figure 1 (b), there are channels running along the *b* axis. The overall free voids are 35.0% of the cell volume, omitting solvent molecules and hydrogen atoms.

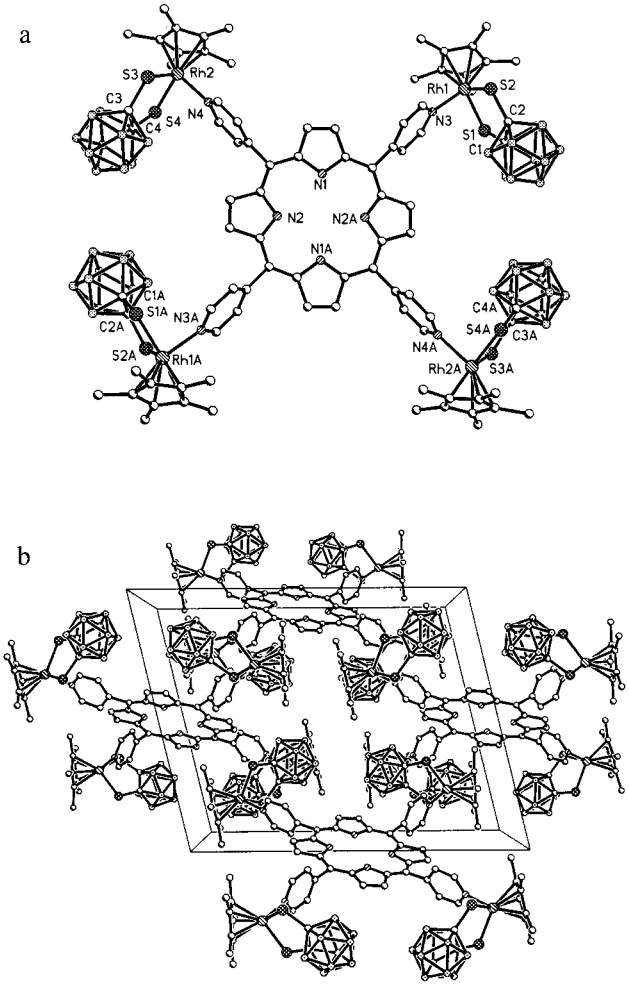

Figure 1. (a) Molecular unit of $[Cp^*RhS_2C_2(B_{10}H_{10})]_4(H_2TPyP)$ (**2a**). (b) Stacking of the molecules in crystals of **2a**, as viewed along the *b* axis. Selected distances [Å] and angles [°]: Rh(1)–N(3) 2.127(7), Rh(1)–S(1) 2.358(3), Rh(1)–S(2) 2.360(3), Rh(2)–N(4) 2.134(7), Rh(2)–S(4) 2.353(3), Rh(2)–S(3) 2.357(3), S(4)–C(4) 1.803(10), S(1)–C(1) 1.788(10), S(2)–C(2) 1.769(11), S(3)–C(3) 1.795(11), C(1)–C(2) 1.655(14), C(3)–C(4) 1.658(14); N(3)–Rh(1)–S(1) 89.3(2), N(3)–Rh(1)–S(2) 89.7(2), S(1)–Rh(1)–S(2) 90.62(10), N(4)–Rh(2)–S(4) 88.6(2), N(4)–Rh(2)–S(3) 91.9(2), S(4)–Rh(2)–S(3) 90.28(10), C(4)–S(4)–Rh(2) 106.4(3), C(1)–S(1)–Rh(1) 105.7(3), C(2)–S(2)–Rh(1) 106.0(3), C(3)–S(3)–Rh(2) 106.3(3).

Changing the ligand from H_2TPyP to tpt gives **3a**, whose structure was established by X-ray structure analysis (Figure 2) and is very similar to that of $[Cp^*IrS_2C_2(B_{10}H_{10})]_3(tpt)$.[6] Three $[Cp^*RhS_2C_2(B_{10}H_{10})]$ units are symmetrically arranged around the periphery of one tpt core to form a "bowl-shaped" structure. All of the rhodium centers adopt a three-legged piano-stool conformation, which has six-coordinate geometry, assuming that the Cp* ligand functions as a three-coordinate ligand. The Rh–N bond lengths are 2.125(6)–2.144(9) Å, which are similar to those of **2a**. Each tpt ligand connects three Rh atoms related by crystallographic threefold symmetry in the tetragonal space group $P4_2/ncm$. It is interesting that the tpt ligand acts in a bifunctional tridentate fashion in **3a** through three N-donor atoms of the oligopyridyl and one triazine group. Two

neighboring molecules of **3a** are paired and staggered in a face-to-face fashion, with the separation between the central triazine rings being 3.46 Å, which is indicative of the presence of π–π stacking interactions. The two neighboring molecules within the stack are rotated by about 60° with respect to each other, just like two buckled bowls.

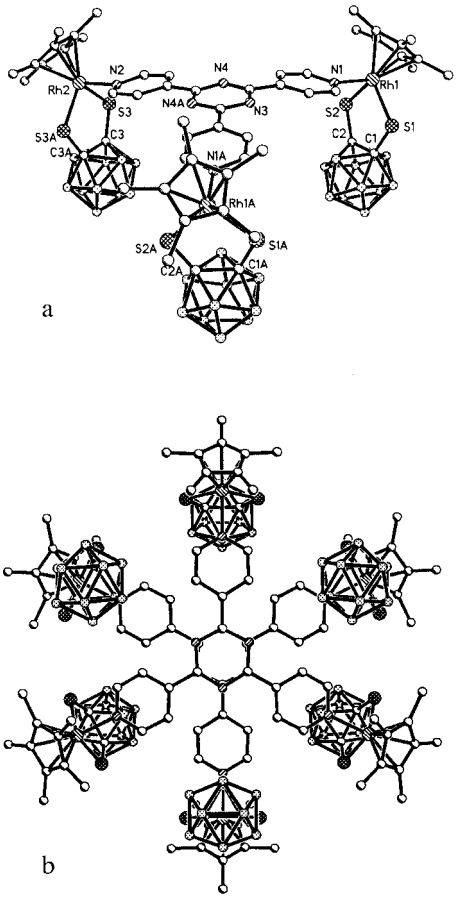

Figure 2. (a) Molecular unit of $[Cp^*RhS_2C_2(B_{10}H_{10})]_3(tpt)$ (**3a**). (b) Two units of **3a** in a staggered disposition. Selected distances [Å] and angles [°]: Rh(1)–N(1) 2.125(6), Rh(1)–S(1) 2.361(2), Rh(1)–S(2) 2.371(2), Rh(2)–N(2) 2.144(9), Rh(2)–S(3a) 2.360(3), Rh(2)–S(3) 2.360(3), S(1)–C(1) 1.765(8), S(2)–C(2) 1.776(8), S(3)–C(3) 1.760(11), C(1)–C(2) 1.690(12), C(3)–C(3a) 1.65(2); N(1)–Rh(1)–S(1) 90.72(18), N(1)–Rh(1)–S(2) 90.54(17), S(1)–Rh(1)–S(2) 91.05(8), N(2)–Rh(2)–S(3a) 90.0(2), N(2)–Rh(2)–S(3) 90.0(2), S(3a)–Rh(2)–S(3) 90.66(15), C(1)–S(1)–Rh(1) 106.0(3), C(2)–S(2)–Rh(1) 105.8(3), C(3)–S(3)–Rh(2) 105.7(4); symmetry transformation for the generation of equivalent atoms *a*: $-x+2, -y, -z+1$.

Another remarkable feature of **3a** is the packing pattern along the *c* axis. These "buckled bowls" stack along the *c* axis to form an interesting stacking structure. As shown in Figure 3, each of the eight molecules of **3a** is paired up to form two types of channels with the dimensions ranging from 3.6–4.0 Å. In other words, each molecule of **3a** is locked into position by pairing up with neighboring molecules in the crystal lattice. The packing in the crystals is such as to create infinite tunnels. It is interesting that such channels are constructed with a double-stranded helix, which consists of repeating "buckled bowl" molecules. Overall, the free voids form 40.1% of the cell volume, omitting hydrogen atoms.

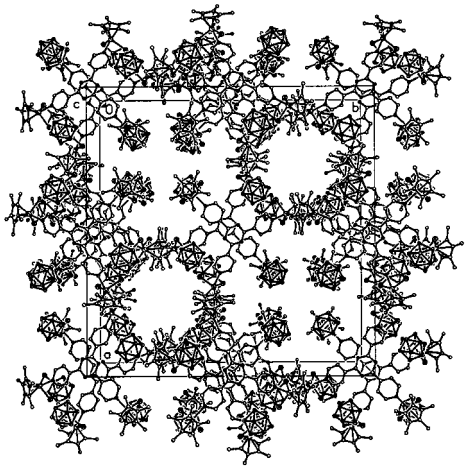

Figure 3. Crystal structure of **3a** viewed down the *c* axis. All hydrogen atoms have been omitted for clarity.

A perspective drawing of **4a** is given in Figure 4. The crystal unit has a crystallographically imposed inversion center in the middle of the Rh···Rh vector. The molecule has a dimeric structure connected by a 4,4′-azopyridine ligand. The plane of the rhodacycle has a dihedral angle of

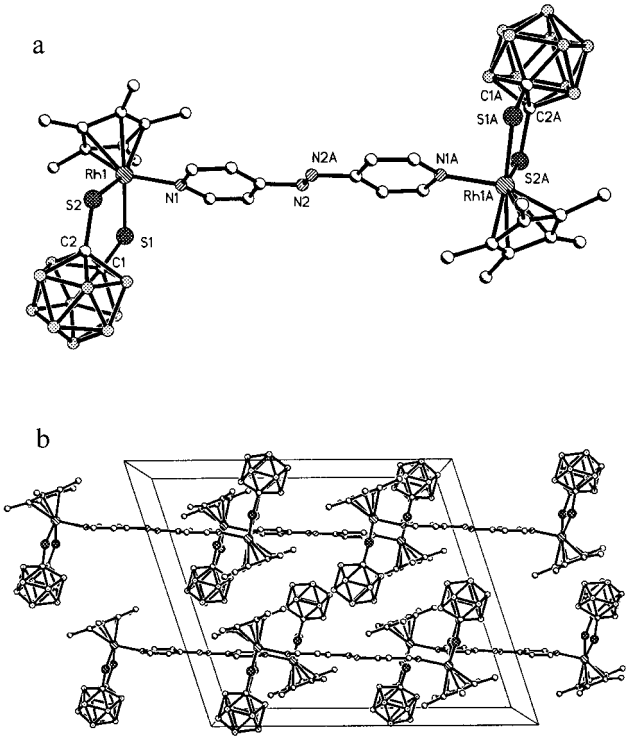

Figure 4. (a) Molecular unit of $[Cp^*Rh\{S_2C_2(B_{10}H_{10})\}]_2(C_{10}H_8N_4)$ (**4a**). (b) Crystal structure of **4a** viewed down the *b* axis. Selected distances [Å] and angles [°]: Rh(1)–N(1) 2.121(3), Rh(1)–S(2) 2.3487(11), Rh(1)–S(1) 2.3526(11), S(1)–C(1) 1.781(4), S(2)–C(2) 1.781(3), C(1)–C(2) 1.658(5); N(1)–Rh(1)–S(2) 90.23(9), N(1)–Rh(1)–S(1) 90.50(9), S(2)–Rh(1)–S(1) 91.06(4), C(1)–S(1)–Rh(1) 105.71(12), C(2)–S(2)–Rh(1) 106.30(13).

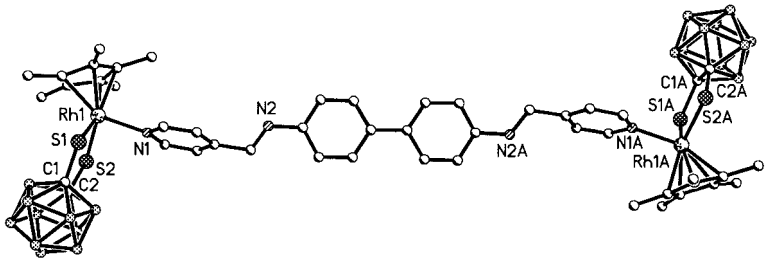

Figure 5. (a) Molecular unit of $[Cp^*Rh\{S_2C_2(B_{10}H_{10})\}]_2(C_{24}H_{18}N_4)$ $2(CHCl_3)$ (**5a**). All hydrogen atoms have been omitted for clarity. Selected distances [Å] and angles [°]: Rh(1)–N(1) 2.140(4), Rh(1)–S(2) 2.3530(17), Rh(1)–S(1) 2.3553(17), S(1)–C(1) 1.778(6), S(2)–C(2) 1.785(6), C(1)–C(2) 1.661(8); N(1)–Rh(1)–S(2) 91.32(14), N(1)–Rh(1)–S(1) 89.90(14), S(2)–Rh(1)–S(1) 91.30(6), C(1)–S(1)–Rh(1) 105.7(2), C(2)–S(2)–Rh(1) 105.7(2).

102.3° with 4,4′-azopyridine, and the Rh···Rh distance is 13.195 Å. Two neighboring molecules of **4a** are staggered in a face-to-face fashion, with the separation between the central Cp* rings being 3.64 Å, which is indicative of the presence of weak π–π stacking interactions (Figure 4, b).

The crystal structures of **5a** and **6a** are similar to that of **4a**, and also consist of $[Cp^*RhS_2C_2(B_{10}H_{10})]$ and *N*,*N*′-bis(4-pyridinylmethylene)biphenyl-4,4′-diamine or pyrazine adducts in a 2:1 molar ratio. As shown in Figures 5 and 6, each Rh is also in a three-legged piano-stool conformation. The Rh–N bond lengths are 2.129(3)–2.140(4) Å, similar to those of **2a**, **3a**, and **4a**. The crystal unit has a crystallographically imposed inversion center in the middle of the Rh···Rh vector. The molecule has a dimeric structure connected by a *N*,*N*′-bis(4-pyridinylmethylene)biphenyl-4,4′-diamine or pyrazine ligand, respectively. The plane of the rhodacycle has a dihedral angle of 100.7° with *N*,*N*′-bis(4-pyridinylmethylene)biphenyl-4,4′-diamine for **5a** and 86.7° with pyrazine for **6a**, and the Rh···Rh distance is 23.980 Å for **5** and 7.019 Å for **6a**.

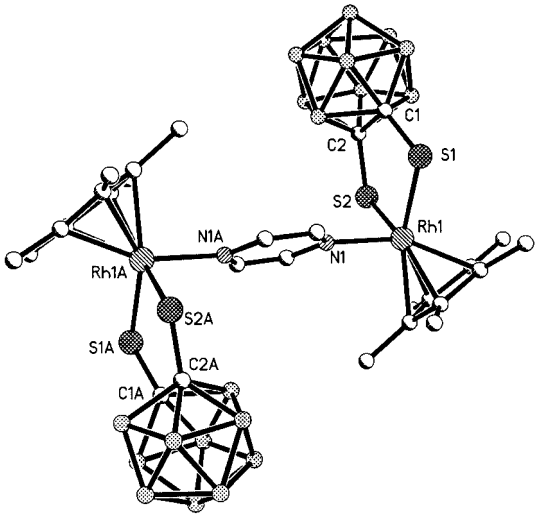

Figure 6. Molecular unit of $[Cp^*Rh\{S_2C_2(B_{10}H_{10})\}]_2(C_4H_4N_2)$ (**6a**). All hydrogen atoms have been omitted for clarity. Selected distances [Å] and angles [°]: Rh(1)–N(1) 2.129(3), Rh(1)–S(2) 2.3528(12), Rh(1)–S(1) 2.3662(12), S(1)–C(1) 1.784(4), S(2)–C(2) 1.769(4),C(1)–C(2), 1.665(5); N(1)–Rh(1)–S(2) 89.32(8), N(1)–Rh(1)–S(1) 91.26(9), S(2)–Rh(1)–S(1) 90.01(5), C(1)–S(1)–Rh(1) 105.97(14).

As shown in Figure 7, there are two crystallographically independent rhodium(III) atoms in the crystal of complex **7a**, and the stoichiometry of $[Cp^*Rh\{S_2C_2(B_{10}H_{10})\}]_2$-$(C_{12}H_8N_4O)$ is 2:1. Each Rh^{III} is also located in a three-legged piano-stool conformation. The two metal atoms Rh(1) and Rh(2) are interconnected by 2,5-di(4-pyridyl)-1,3,5-oxadiazole groups to form a dimeric structure. The plane of each rhodacycle forms a dihedral angle of 88.4° and 91.6° with 2,5-di(4-pyridyl)-1,3,5-oxadiazole, respectively; the Rh(1)···Rh(2) distance is 13.820 Å. It is interesting to note that the two $[Cp^*RhS_2C_2(B_{10}H_{10})]$ fragments

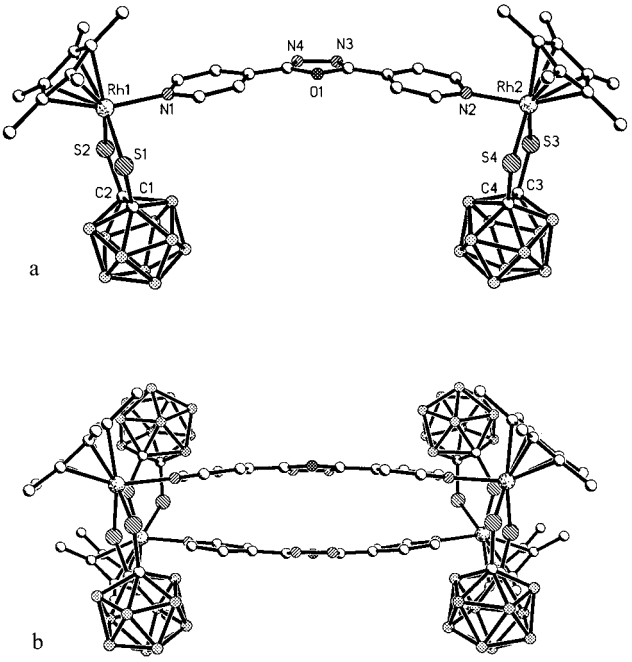

Figure 7. (a) Molecular unit of $[Cp^*Rh\{S_2C_2(B_{10}H_{10})\}]_2$-$(C_{12}H_8N_4O)\cdot(THF)$ (**7a**). (b) Two units of **7a** in a staggered disposition. All hydrogen atoms have been omitted for clarity. Selected distances [Å] and angles [°]: Rh(1)–N(1) 2.148(7), Rh(1)–S(1) 2.356(3), Rh(1)–S(2) 2.363(2), Rh(2)–N(2) 2.126(7), Rh(2)–S(4) 2.343(3), Rh(2)–S(3) 2.369(3), S(1)–C(1) 1.792(9), S(2)–C(2) 1.782(10), S(3)–C(3) 1.785(9), S(4)–C(4) 1.766(9), C(1)–C(2) 1.687(13), C(3)–C(4) 1.637(12); N(1)–Rh(1)–S(1) 91.7(2), N(1)–Rh(1)–S(2) 88.94(19), S(1)–Rh(1)–S(2) 90.38(10), N(2)–Rh(2)–S(4) 91.5(2), N(2)–Rh(2)–S(3) 88.8(2), S(4)–Rh(2)–S(3) 90.30(9), C(1)–S(1)–Rh(1) 106.7(3), C(2)–S(2)–Rh(1) 107.2(3), C(3)–S(3)–Rh(2) 105.7(3), C(4)–S(4)–Rh(2) 106.6(3).

are in a *cis* conformation, which is different from the *trans* conformation in **4a**, **5a**, and **6a**. It is also interesting that the 2,5-bis(4-pyridyl-1,3,5-oxadiazole) ligand is bifunctional didentate in **7a** through two N-donor atoms of the oligopyridyl and one oxadiazole group. Two neighboring molecules of **7a** are paired and staggered in a face-to-face fashion, with the separation between the central oxadiazole rings being 3.15 Å, which is indicative of the presence of strong π–π stacking interactions (Figure 7, b). The two neighboring molecules within the stack are rotated by about 180° with respect to each other, just like two buckled boxes.

The crystal structures of complexes **8b** and **9b** are quite similar to those of **4a**, **5a**, and **6a**. As shown in Figures 8 and 9, respectively, X-ray crystallographic analysis reveals that the complexes are dimers bridged by pyridyl ligands with an Ir···Ir distance of 13.461 Å for **8b** and 19.654 Å for **9b**. The plane of the iridacycle forms a dihedral angle with the pyridyl ring of 107.7° for **8b** and 97.5° for **9b**. It is interesting to note that the two [Cp*IrS$_2$C$_2$(B$_{10}$H$_{10}$)] fragments in **8b** and **9b** are in a *trans* conformation, similar to **4a**, **5a**, and **6a**.

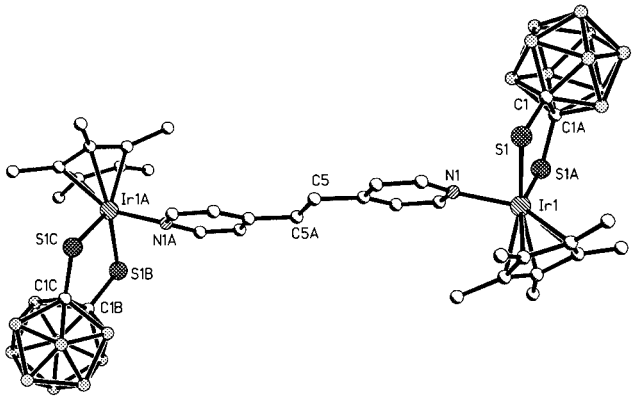

Figure 8. Molecular unit of [Cp*IrS$_2$C$_2$(B$_{10}$H$_{10}$)]$_2$(C$_{12}$H$_{10}$N$_2$) (**8b**). All hydrogen atoms have been omitted for clarity. Selected distances [Å] and angles [°]: Ir(1)–N(1) 2.115(5), Ir(1)–S(1) 2.3568(14), S(1)–C(1) 1.774(5), C(1)–C(1a) 1.662(10); N(1)–Ir(1)–S(1) 87.70(11), N(1)–Ir(1)–S(1a) 87.70(11), S(1)–Ir(1)–S(1a) 90.79(7), C(1)–S(1)–Ir(1) 105.50(17).

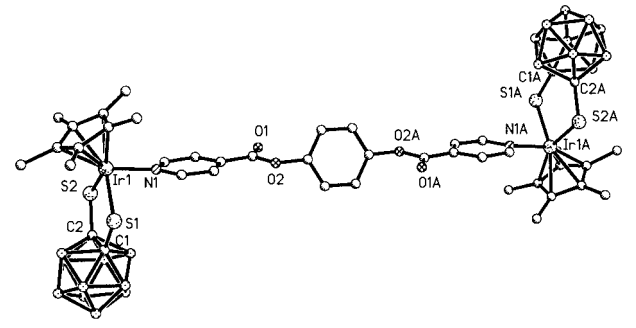

Figure 9. Molecular unit of [Cp*IrS$_2$C$_2$(B$_{10}$H$_{10}$)]$_2$(C$_{18}$H$_{12}$N$_2$O$_4$)·2(CH$_2$Cl$_2$) (**9b**). All hydrogen atoms have been omitted for clarity. Selected distances [Å] and angles [°]: Ir(1)–N(1) 2.132(8), Ir(1)–S(2) 2.3551(18), Ir(1)–S(1) 2.359(3), S(1)–C(1) 1.782(8), S(2)–C(2) 1.768(10), C(1)–C(2) 1.652(13); N(1)–Ir(1)–S(2) 90.35(17), N(1)–Ir(1)–S(1) 88.2(3), S(2)–Ir(1)–S(1) 90.71(7), C(1)–S(1)–Ir(1) 106.3(3), C(2)–S(2)–Ir(1) 105.6(3).

In summary, a new set of multi-cluster molecules has been synthesized from half-sandwich rhodium(III) and iridium(III) complexes bearing 1,2-dicarba-*closo*-dodecaborane(12)-1,2-dithiolate chelate ligands and different multidentate pyridyl ligands. This synthetic approach, which is based upon stepwise building-up of metal clusters with organic fragments, offers the potential for exquisite control over the detailed architecture of the materials, which may lead to a variety of unusual shapes.

Experimental Section

All manipulations were performed under nitrogen using standard Schlenk techniques or in a glove box. Solvents were dried by refluxing over sodium/benzophenone ketyl (toluene, hexane, cyclohexane) and distilled just before use. [Cp*Rh{S$_2$C$_2$(B$_{10}$H$_{10}$)}] (**1a**),[12] [Cp*Ir{S$_2$C$_2$(B$_{10}$H$_{10}$)}] (**1b**),[13] 2,4,6-tri(4-pyridyl)-1,3,5-triazine,[14] 4,4′-azopyridine,[15] *N*,*N*′-bis(4-pyridinylmethylene)biphenyl-4,4′-diamine,[16] diisonicotinic acid 1,4-phenylene diester,[17] 2,5-di(4-pyridyl)-1,3,4-oxadiazole[18] were prepared by methods reported previously. IR spectra were recorded with a Nicolet AVATAR-360IR spectrometer, whereas ^{1}H (500 MHz) and ^{11}B (160 MHz) NMR spectra were obtained with a Bruker DMX-500 spectrometer in CDCl$_3$ solution. Elemental analyses were performed with an Elementar vario EI Analyzer.

Caution! *Perchlorate salts are explosive (especially when dry) and should be handled with care.*

Synthesis of [Cp*Rh{S$_2$C$_2$(B$_{10}$H$_{10}$)}]$_4$(H$_2$TPyP) (2a): A mixture of **1a** (178 mg, 0.4 mmol) and H$_2$TpyP (62 mg, 0.1 mmol) in CH$_2$Cl$_2$ (30 mL) was stirred for 24 h, whereupon the green-colored mixture gradually changed to red. The solvent was then evaporated under vacuum. The residue was washed with toluene to give a violet solid of **2a** (190 mg, 79%). C$_{88}$H$_{126}$B$_{40}$N$_8$Rh$_4$S$_8$ (2396.6): calcd. C 44.10, H 5.30, N 4.68; found C 43.85, H 5.16, N 4.57. ^{1}H NMR (500 MHz, CDCl$_3$, 20 °C): δ = –2.89 (s, porphine NH, 2 H), 1.78 (s, C$_5$Me$_5$, 60 H), 8.20 (d, $^3J_{H,H}$ = 5 Hz, 3,5-pyridyl, 8 H), 9.02 (m, pyrrole, 8 H), 9.38 (d, $^3J_{H,H}$ = 5 Hz, 2,6-pyridyl, 8 H) ppm. ^{11}B NMR (160 MHz, CDCl$_3$, 20 °C): δ = –5.8, –8.2, –9.0, –10.8 ppm. IR (KBr pellet): $\tilde{\nu}$ = 2581, 2559 (ν_{B-H}), 1578, 1420, 986, 792 cm^{-1}.

Synthesis of [Cp*Rh{S$_2$C$_2$(B$_{10}$H$_{10}$)}]$_3$(C$_{18}$H$_{12}$N$_6$) (3a): A solution of **1a** (133 mg, 0.3 mmol) in CH$_2$Cl$_2$ (30 mL) was added to tpt (31 mg, 0.1 mmol) in CH$_2$Cl$_2$ (30 mL). The green-colored mixture was stirred for 24 h, whereupon it gradually changed to violet. The solvent was then evaporated under vacuum. The residue was washed with toluene to give a violet solid of **3a** (143 mg, 82%). C$_{54}$H$_{87}$B$_{30}$N$_6$Rh$_3$S$_6$ (1645.8): calcd. C 39.41, H 5.33, N 5.11; found C 39.28, H 5.27, N 5.10. ^{1}H NMR (500 MHz, CDCl$_3$, 20 °C): δ = 1.77 (s, 30 H, C$_5$Me$_5$), 8.67 (br., 6 H, 3,5-pyridyl), 8.96 (br., 6 H, 2,6-pyridyl) ppm. ^{11}B NMR (160 MHz, CDCl$_3$, 20 °C): δ = –7.9, –10.3 ppm. IR (KBr pellet): $\tilde{\nu}$ = 2573, 2559 cm^{-1} (ν_{B-H}).

Synthesis of [Cp*Rh{S$_2$C$_2$(B$_{10}$H$_{10}$)}]$_2$(C$_{10}$H$_8$N$_4$) (4a): A solution of **1a** (89 mg, 0.2 mmol) in CH$_2$Cl$_2$ (30 mL) was added to 4,4′-azopyridine (21 mg, 0.1 mmol) in CH$_2$Cl$_2$ (30 mL). The green-colored mixture was stirred for 24 h, whereupon it gradually became dark red. The solvent was then evaporated under vacuum. The residue was washed with toluene to give a red solid of **4a** (85 mg, 79%).

$C_{34}H_{58}B_{20}N_4Rh_2S_4$ (1073.1): calcd. C 38.05, H 5.45, N 5.22; found C 37.87, H 5.39, N 5.17. ^{1}H NMR (500 MHz, $CDCl_3$, 20 °C): δ = 1.77 (s, 30 H, C_5Me_5), 7.76 (d, $^3J_{H,H}$ = 5 Hz, 4 H, 3,5-pyridyl), 8.85 (d, $^3J_{H,H}$ = 5 Hz, 4 H, 2,6-pyridyl) ppm. ^{11}B NMR (160 MHz, $CDCl_3$, 20 °C): δ = –6.1, –7.5, –8.7, –10.9 ppm. IR (KBr pellet): $\tilde{\nu}$ = 2568 (ν_{B-H}), 1657, 1600, 1491, 1450 cm^{-1}.

Synthesis of [Cp*Ir{$S_2C_2(B_{10}H_{10})$}]$_2$($C_{10}H_8N_4$) (4b): A solution of **1b** (106 mg, 0.2 mmol) in CH_2Cl_2 (30 mL) was added to 4,4′-azopyridine (21 mg, 0.1 mmol) in CH_2Cl_2 (30 mL). The blue-colored mixture was stirred for 24 h, whereupon it gradually became dark red. The solvent was then evaporated under vacuum. The residue was washed with toluene to give a red solid of **4b** (100 mg, 80%). $C_{34}H_{58}B_{20}Ir_2N_4S_4$ (1251.8): calcd. C 32.62, H 4.67, N 4.48; found C 32.39, H 4.61, N 4.43. ^{1}H NMR (500 MHz, $CDCl_3$, 20 °C): δ = 1.87 (s, 30 H, C_5Me_5), 7.80 (d, $^3J_{H,H}$ = 5 Hz, 4 H, 3,5-pyridyl), 8.92 (d, $^3J_{H,H}$ = 5 Hz, 4 H, 2,6-pyridyl) ppm. ^{11}B NMR (160 MHz, $CDCl_3$, 20 °C): δ = –6.2, –7.5, –8.6, –10.5 ppm. IR (KBr pellet): $\tilde{\nu}$ = 2562 (ν_{B-H}), 1653, 1610, 1491, 1438 cm^{-1}.

Synthesis of [Cp*Rh{$S_2C_2(B_{10}H_{10})$}]$_2$($C_{24}H_{18}N_4$) (5a): A solution of **1a** (89 mg, 0.2 mmol) in CH_2Cl_2 (30 mL) was added to *N*,*N*′-bis(4-pyridinylmethylene)biphenyl-4,4′-diamine (36 mg, 0.1 mmol) in CH_2Cl_2 (30 mL). The green-colored mixture was stirred for 24 h, whereupon it gradually became dark red. The solvent was then evaporated under vacuum. The residue was washed with toluene to give a red solid of **5a** (91 mg, 73%). $C_{48}H_{68}B_{20}N_4Rh_2S_4$ (1251.4): calcd. C 46.07, H 5.48, N 4.48; found C 45.77, H 5.39, N 4.41. ^{1}H NMR (500 MHz, $CDCl_3$, 20 °C): δ = 1.76 (s, 30 H, C_5Me_5), 7.2–7.5 (m, 8 H, biphenyl), 7.69 (s, 2 H, CH), 8.25 (br., 4 H, 3,5-pyridyl), 9.12 (br., 4 H, 2,6-pyridyl) ppm. ^{11}B NMR (160 MHz, $CDCl_3$, 20 °C): δ = –6.1, –7.5, –8.9, –10.6, –12.2 ppm. IR (KBr pellet): $\tilde{\nu}$ = 2551, 2573 cm^{-1}(ν_{B-H}).

Synthesis of [Cp*Rh{$S_2C_2(B_{10}H_{10})$}]$_2$($C_4H_4N_2$) (6a): A solution of **1a** (178 mg, 0.4 mmol) in CH_2Cl_2 (30 mL) was added to pyrazine (17 mg, 0.2 mmol) in CH_2Cl_2 (30 mL). The green-colored mixture was stirred for 24 h, whereupon it gradually became dark red. The solvent was then evaporated under vacuum. The residue was washed with toluene to give a red solid of **6a** (159 mg, 82%). $C_{28}H_{54}B_{20}N_2Rh_2S_4$ (969.03): calcd. C 34.70, H 5.62, N 2.89; found C 34.59, H 5.58, N 2.83. ^{1}H NMR (500 MHz, $CDCl_3$, 20 °C): δ = 1.79 (s, 30 H, C_5Me_5), 8.80 (s, 4 H, pyrazine) ppm. ^{11}B NMR (160 MHz, $CDCl_3$, 20 °C): δ = –7.7, –10.2 ppm. IR (KBr pellet): $\tilde{\nu}$ = 2563 cm^{-1} (ν_{B-H}).

Synthesis of [Cp*Ir{$S_2C_2(B_{10}H_{10})$}]$_2$($C_4H_4N_2$) (6b): A solution of **1b** (213 mg, 0.4 mmol) in CH_2Cl_2 (30 mL) was added to pyrazine (17 mg, 0.2 mmol) in CH_2Cl_2 (30 mL). The green-colored mixture was stirred for 24 h, whereupon it gradually became dark red. The solvent was then evaporated under vacuum. The residue was washed with toluene to give a red solid of **6b** (197 mg, 86%). $C_{28}H_{54}B_{20}Ir_2N_2S_4$ (1147.66): calcd. C 29.30, H 4.74, N 2.44; found C 29.01, H 4.71, N 2.42. ^{1}H NMR (500 MHz, $CDCl_3$, 20 °C): δ = 1.86 (s, 30 H, C_5Me_5), 8.81 (s, 4 H, pyrazine) ppm. ^{11}B NMR (160 MHz, $CDCl_3$, 20 °C): δ = –7.3, –10.1 ppm. IR (KBr pellet): $\tilde{\nu}$ = 2558 cm^{-1} (ν_{B-H})

Synthesis of [Cp*Rh{$S_2C_2(B_{10}H_{10})$}]$_2$($C_{12}H_8N_4O$) (7a): A solution of **1a** (89 mg, 0.2 mmol) in CH_2Cl_2 (30 mL) was added to 2,5-di(4-pyridyl)-1,3,5-oxadiazole (22 mg, 0.1 mmol) in CH_2Cl_2 (30 mL). The green-colored mixture was stirred for 24 h, whereupon it gradually became dark red. The solvent was then evaporated under vacuum. The residue was washed with toluene to give a red solid of **7a** (86 mg, 77%). $C_{36}H_{58}B_{20}N_4ORh_2S_4$ (1113.2): calcd. C 38.84, H 5.25, N 5.03; found C 38.49, H 5.17, N 4.98. ^{1}H NMR (500 MHz, $CDCl_3$, 20 °C): δ = 1.76 (s, 30 H, C_5Me_5), 7.67 (d, $^3J_{H,H}$ = 5 Hz, 4 H, 3,5-pyridyl), 8.76 (d, $^3J_{H,H}$ = 5 Hz, 4 H, 2,6-pyridyl) ppm. ^{11}B NMR (160 MHz, $CDCl_3$, 20 °C): δ = –5.7, –7.3, –8.9, –10.6 ppm. IR (KBr pellet): $\tilde{\nu}$ = 2555, 2576 cm^{-1} (ν_{B-H}).

Synthesis of [Cp*Rh{$S_2C_2(B_{10}H_{10})$}]$_2$($C_{12}H_{10}N_2$) (8a): A solution of **1a** (89 mg, 0.2 mmol) in CH_2Cl_2 (30 mL) was added to 1,2-di(4-pyridyl)ethylene (18 mg, 0.1 mmol) in CH_2Cl_2 (30 mL). The green-colored mixture was stirred for 24 h, whereupon it gradually became dark red. The solvent was then evaporated under vacuum. The residue was washed with toluene to give a red solid of **8a** (76 mg, 71%). $C_{36}H_{60}B_{20}Rh_2N_2S_4$ (1071.2): calcd. C 40.37, H 5.65, N 2.62; found C 40.19, H 5.53, N 2.55. ^{1}H NMR (500 MHz, $CDCl_3$, 20 °C): δ = 1.77 (s, 30 H, C_5Me_5), 7.20 (m, 2 H, CH), 7.56 (br., 4 H, 3,5-pyridyl), 8.81 (m, 4 H, 2,6-pyridyl) ppm. ^{11}B NMR (160 MHz, $CDCl_3$, 20 °C): δ = –5.8, –7.2, –8.5, –10.3 ppm. IR (KBr pellet): $\tilde{\nu}$ = 2559, 2580 cm^{-1} (ν_{B-H}).

Synthesis of [Cp*Ir{$S_2C_2(B_{10}H_{10})$}]$_2$($C_{12}H_{10}N_2$) (8b): A solution of **1b** (106 mg, 0.2 mmol) in CH_2Cl_2 (30 mL) was added to 1,2-di(4-pyridyl)ethylene (18 mg, 0.1 mmol) in CH_2Cl_2 (30 mL). The blue-colored mixture was stirred for 24 h, whereupon it gradually became dark red. The solvent was then evaporated under vacuum. The residue was washed with toluene to give a red solid of **8b** (94 mg, 75%). $C_{36}H_{60}B_{20}Ir_2N_2S_4$ (1249.8): calcd. C 34.60, H 4.84, N 2.24; found C 34.31, H 4.79, N 2.21. ^{1}H NMR (500 MHz, $CDCl_3$, 20 °C): δ = 1.87 (s, C_5Me_5, 30 H), 7.26 (m, CH, 2 H), 7.71 (br., pyridyl, 4 H), 8.92 (br., pyridyl, 4 H) ppm. ^{11}B NMR (160 MHz, $CDCl_3$, 20 °C): δ = –5.9, –7.1, –8.5, –10.5 ppm. IR (KBr pellet): $\tilde{\nu}$ = 2561, 2579 cm^{-1} (ν_{B-H}).

Synthesis of [Cp*Rh{$S_2C_2(B_{10}H_{10})$}]$_2$($C_{18}H_{12}N_2O_4$) (9a): A solution of **1a** (89 mg, 0.2 mmol) in CH_2Cl_2 (30 mL) was added to diisonicotinic acid 1,4-phenylene diester (32 mg, 0.1 mmol) in CH_2Cl_2 (30 mL). The green-colored mixture was stirred for 24 h, whereupon it gradually became dark red. The solvent was then evaporated under vacuum. The residue was washed with toluene to give a red solid of **9a** (98 mg, 81%). $C_{42}H_{62}B_{20}N_2O_4Rh_2S_4$ (1209.2): calcd. C 41.72, H 5.17, N 2.32; found C 41.59, H 5.08, N 2.25. ^{1}H NMR (500 MHz, $CDCl_3$, 20 °C): δ = 1.78 (s, C_5Me_5, 20 H), 7.26 (s, phenyl, 4 H), 7.79 (d, $^3J_{H,H}$ = 5 Hz, 4 H, 3,5-pyridyl), 8.95 (s, $^3J_{H,H}$ = 5 Hz, 4 H, 2,6-pyridyl) ppm. ^{11}B NMR (160 MHz, $CDCl_3$, 20 °C): δ = –3.2, –5.3, –7.0, –8.2, –9.7, –12.8 ppm (signal overlap). IR (KBr pellet): $\tilde{\nu}$ = 2563, 2575 cm^{-1} (ν_{B-H}), 1692 ($\nu_{C=O}$).

Synthesis of [Cp*Ir{$S_2C_2(B_{10}H_{10})$}]$_2$($C_{18}H_{12}N_2O_4$) (9b): A solution of **1b** (106 mg, 0.2 mmol) in CH_2Cl_2 (30 mL) was added to diisonicotinic acid 1,4-phenylene diester (32 mg, 0.1 mmol) in CH_2Cl_2 (30 mL). The blue-colored mixture was stirred for 24 h, whereupon it gradually became dark red. The solvent was then evaporated under vacuum. The residue was washed with toluene to give a red solid of **9b** (115 mg, 83%). $C_{42}H_{62}B_{20}Ir_2N_2O_4S_4$ (1387.9): calcd. C 36.35, H 4.50, N 2.02; found C 36.07, H 4.39, N 1.93. ^{1}H NMR (500 MHz, $CDCl_3$, 20 °C): δ = 1.89 (s, C_5Me_5, 20 H), 7.31 (s, phenyl, 4 H), 7.89 (d, $^3J_{H,H}$ = 5 Hz, 4 H, 3,5-pyridyl), 9.01 (d, $^3J_{H,H}$ = 5 Hz, 4 H, 2,6-pyridyl) ppm. ^{11}B NMR (160 MHz, $CDCl_3$, 20 °C): δ = –3.2, –5.3, –7.0, –8.2, –9.7, –12.8 ppm (signal overlap). IR (KBr pellet): $\tilde{\nu}$ = 2562, 2575 cm^{-1} (ν_{B-H}), 1690 ($\nu_{C=O}$).

Synthesis of [Cp*Rh{$S_2C_2(B_{10}H_{10})$}]($C_{10}H_8N_2$) (10a): A solution of **1a** (89 mg, 0.2 mmol) in CH_2Cl_2 (30 mL) was added to 4,4′-bipyridine (16 mg, 0.1 mmol) in CH_2Cl_2 (30 mL). The green-colored mixture was stirred for 24 h, whereupon it gradually became dark red. The solvent was then evaporated under vacuum. The residue was washed with toluene to give a red solid of **10a** (85 mg, 81%). $C_{34}H_{58}B_{20}N_2Rh_2S_4$ (1045.1): calcd. C 39.07, H 5.59, N 2.68; found C 38.92, H 5.46, N 2.60. ^{1}H NMR (500 MHz, $CDCl_3$, 20 °C): δ = 1.78 (s, C_5Me_5, 30 H), 7.53 (d, $^3J_{H,H}$ = 5 Hz, 2,6-pyridyl, 4 H),

8.71 (d, $^3J_{H,H}$ = 5 Hz, 3,5-pyridyl, 4 H) ppm. ^{11}B NMR (160 MHz, $CDCl_3$, 25 °C): δ = –6.5, –7.7, –8.1, –10.8 ppm. IR (KBr pellet): $\tilde{\nu}$ = 2582, 2571 cm^{-1} (ν_{B-H}).

Synthesis of [Cp*Ir{$S_2C_2(B_{10}H_{10})$}]($C_{10}H_8N_2$) (10b): A solution of **1b** (106 mg, 0.2 mmol) in CH_2Cl_2 (30 mL) was added to 4,4′-bipyridine (16 mg, 0.1 mmol) in CH_2Cl_2 (30 mL). The blue-colored mixture was stirred for 24 h, whereupon it gradually became dark red. The solvent was then evaporated under vacuum. The residue was washed with toluene to give a red solid of **10b** (106 mg, 87%). $C_{34}H_{58}B_{20}Ir_2N_2S_4$ (1223.75): calcd. C 33.37, H 4.78, N 2.29; found C 32.98, H 4.57, N 2.23. ^{1}H NMR (500 MHz, $CDCl_3$, 20 °C): δ = 1.86 (s, C_5Me_5, 30 H), 7.57 (d, $^3J_{H,H}$ = 5 Hz, 3,5-pyridyl, 4 H), 8.77 (d, $^3J_{H,H}$ = 5 Hz, 2,6-pyridyl, 4 H) ppm. ^{11}B NMR (160 MHz, $CDCl_3$, 25 °C): δ = –6.3, –8.1, –8.7, –10.3 ppm. IR (KBr pellet): $\tilde{\nu}$ = 2583, 2571 cm^{-1} (ν_{B-H}).

X-ray Crystallographic Analysis: Diffraction intensity data were collected with a Bruker Smart Apex CCD diffractometer. The determination of the unit cell and the collection of intensity data were performed with graphite-monochromated Mo-K_α radiation (λ = 0.71073 Å). All the data were collected at room temperature using the ω-scan technique. The structures were solved by direct methods using Fourier techniques, and refined on F^2 by a full-matrix least-squares method. SADABS[19] absorption corrections were applied to the data. All non-hydrogen atoms were refined with anisotropic

Table 1. Crystallographic data for compounds **2a**, **3a**, and **4a**.

	2a	**3a**	**4a**
Empirical formula	$C_{47}H_{68}B_{20}Cl_6N_4Rh_2S_4$	$C_{54}H_{87}B_{30}N_6Rh_3S_3$	$C_{34}H_{58}B_{20}N_4Rh_2S_4$
M	1452.01	1645.68	1073.10
Crystal size [mm]	0.20×0.18×0.15	0.36×0.25×0.18	0.15×0.12×0.10
Crystal system	monoclinic	tetragonal	monoclinic
Space group	$P2_1/n$	$P4_2/n$cm	$C2/c$
a [Å]	17.054(5)	35.361(8)	18.589(6)
b [Å]	19.400(6)	35.361(8)	13.115(4)
c [Å]	21.333(6)	16.106(5)	21.696(8)
β [°]	103.470(5)		107.890(5)
V [Å^3]	6864(3)	20139(9)	5034(3)
Z	4	8	4
$\rho_{calcd.}$ [g cm^{-3}]	1.405	1.086	1.416
μ(Mo-K_α) [mm^{-1}]	0.872	0.642	0.854
Collected reflections	28432	81749	12471
Unique	12021	9069	5506
Parameters	748	464	304
Goodness of fit	1.040	1.092	0.779
R_1[a] [$I > 2\sigma(I)$]	0.0928	0.0835	0.0404
wR_2[a] [$I > 2\sigma(I)$]	0.2144	0.2436	0.0639
Max./min. residual density [e Å^{-3}]	2.006/–0.812	1.144/–0.502	0.575/–0.430

[a] $R_1 = \Sigma||F_o|-|F_c||$ (based on reflections with $F_o^2 > 2\sigma F^2$). $wR_2 = [\Sigma\{w(F_o^2-F_c^2)^2\}/\Sigma\{w(F_o^2)^2\}]^{1/2}$; $w = 1/[\sigma^2(F_o^2)+(0.095P)^2]$; $P = [\max(F_o^2, 0)+2F_c^2]/3$ (also with $F_o^2 > 2\sigma F^2$).

Table 2. Crystallographic data for compounds **5a**, **6a**, and **7a**.

	5a	**6a**	**7a**
Empirical formula	$C_{25}H_{37}B_{10}Cl_3N_2RhS_2$	$C_{28}H_{54}B_{20}N_2Rh_2S_4$	$C_{40}H_{62}B_{20}N_4O_2Rh_2S_4$
M	747.05	968.99	1181.20
Crystal size	0.20×0.16×0.10	0.20×0.15×0.10	0.10×0.10×0.08
Crystal system	monoclinic	triclinic	monoclinic
Space group	$P2_1/n$	$P\bar{1}$	$P2_1/c$
a [Å]	11.530(2)	8.0300(16)	12.213(4)
b [Å]	12.845(3)	11.270(2)	18.241(6)
c [Å]	24.066(5)	13.560(3)	25.984(8)
α [°]		95.82(3)	
β [°]	99.272(3)	90.96(3)	94.340(6)
γ [°]		109.54(3)	
V [Å^3]	3517.7(12)	1148.8(4)	5772(3)
Z	4	1	4
$\rho_{calcd.}$ [g cm^{-3}]	1.411	1.401	1.359
μ(Mo-K_α) [mm^{-1}]	0.853	0.926	0.754
Collected reflections	14548	4868	24082
Unique	6213	4000	10171
Parameters	398	268	654
Goodness of fit	1.020	1.038	0.704
R_1[a] [$I > 2\sigma(I)$]	0.0615	0.0371	0.0520
wR_2[a] [$I > 2\sigma(I)$]	0.1395	0.0857	0.1141
Max./min. residual density [e Å^{-3}]	0.905/–0.578	0.338/–0.440	0.996/–0.472

[a] $R_1 = \Sigma||F_o|-|F_c||$ (based on reflections with $F_o^2 > 2\sigma F^2$). $wR_2 = [\Sigma\{w(F_o^2-F_c^2)^2\}/\Sigma\{w(F_o^2)^2\}]^{1/2}$; $w = 1/[\sigma^2(F_o^2)+(0.095P)^2]$; $P = [\max(F_o^2, 0)+2F_c^2]/3$ (also with $F_o^2 > 2\sigma F^2$).

Table 3. Crystallographic data for compounds **8b** and **9b**.

	8b	**9b**
Empirical formula	$C_{19}H_{32}B_{10}Cl_2IrNS_2$	$C_{44}H_{66}B_{20}Cl_4Ir_2N_2O_4S_4$
M	709.78	1557.63
Crystal size	0.30×0.18×0.15	0.12×0.10×0.06
Crystal system	orthorhombic	orthorhombic
Space group	*Pnnm*	*Pbca*
a [Å]	14.804(4)	17.865(6)
b [Å]	18.493(5)	15.210(5)
c [Å]	10.485(3)	22.950(7)
V [Å^3]	2870.4(14)	6236(3)
Z	4	4
$\rho_{calcd.}$ [g cm^{-3}]	1.642	1.659
μ(Mo-K_α) [mm^{-1}]	4.995	4.611
Collected reflections	11645	5575
Unique	2694	3395
Parameters	200	376
Goodness of fit	1.097	0.719
R_1[a] [$I > 2\sigma(I)$]	0.0303	0.0319
wR_2[a] [$I > 2\sigma(I)$]	0.0799	0.0447
Max./min. residual density [e Å^{-3}]	1.546/–1.030	0.556/–0.570

[a] $R_1 = \Sigma||F_o|-|F_c||$ (based on reflections with $F_o^2 > 2\sigma F^2$). $wR_2 = [\Sigma\{w(F_o^2-F_c^2)^2\}/\Sigma\{w(F_o^2)^2\}]^{1/2}$; $w = 1/[\sigma^2(F_o^2)+(0.095P)^2]$; $P = [\max(F_o^2, 0)+2F_c^2]/3$ (also with $F_o^2 > 2\sigma F^2$).

displacement coefficients, expect the solvent molecules in **2a** and **7a**. Hydrogen atoms were used in calculated positions. All the calculations were carried out using the program SHELXTL.[20] All figures were produced with the PLATON program.[21] Crystal data, data-collection parameters, and the results of the analyses of compounds **2a**, **3a**, and **4a** (Table 1), **5a**, **6a**, and **7a** (Table 2), and **8b** and **9b** (Table 3) are given below.

CCDC-298247, -298248, -298249, -298250, -298251, -298252, -298253, and -298254 contain the supplementary crystallographic data for this paper. These data can be obtained free of charge from The Cambridge Crystallographic Data Center via www.ccdc.cam.ac.uk/data_request/cif.

Acknowledgments

Financial support by the National Nature Science Foundation of China for Distinguished Young Scholars (20531020, 20421303) and the Shanghai Science and Technology Committee (05JC14003, 05DZ22313) is gratefully acknowledged.

[1] a) G.-X. Jin, *Coord. Chem. Rev.* **2004**, *248*, 587–602; b) G.-X. Jin, in *Perspectives in Organometallic Chemistry* (Eds.: C. G. Screttas, B. R. Steele), RSC Press, Cambridge, **2003**, p. 47–63.
[2] a) D. H. Kim, J. Ko, K. Park, S. Cho, S. O. Kang, *Organometallics* **1999**, *18*, 2738–2740; b) X. Hou, X. Wang, J.-Q. Wang, G.-X. Jin, *J. Organomet. Chem.* **2004**, *689*, 2228–2235.
[3] a) J. Pang, E. J. P. Marcotte, C. Seward, R. S. Brown, S. Wang, *Angew. Chem. Int. Ed.* **2001**, *40*, 4042–4045; b) C. Seward, W.-L. Jia, R.-Y. Wang, G. D. Enright, S. Wang, *Angew. Chem. Int. Ed.* **2004**, *43*, 2933–2936; c) W.-L. Jia, R.-Y. Wang, D. Song, S. J. Ball, A. B. Mclean, S. Wang, *Chem. Eur. J.* **2005**, *11*, 832–842.
[4] a) F. A. Cotton, C. Lin, C. A. Murillo, *Acc. Chem. Res.* **2001**, *34*, 759–771; b) B. K. Roland, H. D. Selby, M. D. Carducci, Z. Zheng, *J. Am. Chem. Soc.* **2002**, *124*, 3222–3223; c) B. K. Roland, C. Carter, Z. Zheng, *J. Am. Chem. Soc.* **2002**, *124*, 6234–6235; d) H. D. Selby, B. K. Roland, Z. Zheng, *Acc. Chem. Res.* **2003**, *36*, 933–944.
[5] J.-Q. Wang, C.-X. Ren, L.-H. Weng, G.-X. Jin, *Chem. Commun.* **2006**, 162–164.
[6] J.-Q. Wang, C.-X. Ren, G.-X. Jin, *Chem. Commun.* **2005**, 4738–4740.
[7] a) D. Armspach, M. Cattalini, E. C. Constable, *Chem. Commun.* **1996**, 1823–1864; b) E. C. Constable, *Chem. Commun.* **1997**, 1073–1080.
[8] a) X.-F. Hou, X.-C. Wang, J.-Q. Wang, G.-X. Jin, *J. Organomet. Chem.* **2004**, *689*, 2228–2235; b) Q. Kong, G.-X. Jin, S. Cai, L. Weng, *Chin. Sci. Bull.* **2003**, *48*, 1733–1736.
[9] a) G.-X. Jin, J.-Q. Wang, Z. Zheng, L.-H. Weng, M. Herberhold, *Angew. Chem. Int. Ed.* **2005**, *44*, 259–262; b) J.-Q. Wang, X.-F. Hou, L.-H. Weng, G.-X. Jin, *Organometallics* **2005**, *24*, 826–830; c) J.-Q. Wang, L.-H. Weng, G.-X. Jin, *J. Organomet. Chem.* **2005**, *690*, 249–252.
[10] a) S. Leininger, B. Olenyuk, P. J. Stang, *Chem. Rev.* **2000**, *100*, 853–908; b) G. F. Swiegers, T. J. Malefetse, *Chem. Rev.* **2000**, *100*, 3483–3538; c) J. A. R. Navrro, B. Lippert, *Coord. Chem. Rev.* **2001**, *222*, 219–250.
[11] J.-Q. Wang, C.-X. Ren, G.-X. Jin, *Organometallics* **2006**, *25*, 74–81.
[12] M. Herberhold, G.-X. Jin, H. Yan, W. Milius, B. Wrackmeyer, *J. Organomet. Chem.* **1999**, *587*, 252–257.
[13] M. Herberhold, G.-X. Jin, H. Yan, W. Milius, B. Wrackmeyer, *Eur. J. Inorg. Chem.* **1999**, 873–875.
[14] H. L. Anderson, S. Anderson, J. K. M. Sanders, *J. Chem. Soc., Perkin Trans. 1* **1995**, 2231–2245.
[15] E. V. Brown, G. R. Granneman, *J. Am. Chem. Soc.* **1975**, *97*, 621–627.
[16] J. A. Nash, G. W. Gray, *Mol. Cryst. Liq. Cryst.* **1974**, *25*, 299–321.
[17] X.-B. Shao, X.-K. Jiang, X. Zhao, C.-X. Zhao, Y. Chen, Z.-T. Li, *J. Org. Chem.* **2004**, *69*, 899–907.
[18] Z.-J. Ren, E. Jiang, H.-B. Zhou, *Youji Huaxue* **1995**, *15*, 218–220.
[19] G. M. Sheldrick, *SADABS* (*2.01*), *Bruker*/*Siemens Area Detector Absorption Correction Program*, Bruker AXS, Madison, Wisconsin, USA, **1998**.
[20] G. M. Sheldrick, *SHELXL-97*; University of Gtötingen: Germany, **1997**.
[21] *PLATON*: A multi-purpose crystallographic tool, Utrecht University, The Netherlands. See: A. L. Spek, *Acta Crystallogr., Sect. A* **1990**, *46*, C34.

Received: April 3, 2006
Published Online: June 28, 2006

